Bulletin T.CXLV de l'Académie serbe des sciences et des arts – 2013
Classe des Sciences mathématiques et naturelles
Sciences mathématiques, № 38

PRECISION SPECTROSCOPY USING QUANTUM SUPERPOSITION OF ATOMIC LEVELS

B. M. JELENKOVIĆ

(Presented at the 3rd Meeting, held on April 26, 2013)

1. *Introduction*

In quantum mechanics there is a possibility for superposition of two quantum states $|\psi_1\rangle = \sum_n c_n^1 |n>$ and $|\psi_2\rangle = \sum_n c_n^2 |n>$, given as $\frac{1}{\sqrt{2}}(|\psi_1\rangle + |\psi_2\rangle)$. Such superposition has the unique property - a probability of beiing in state $|n\rangle$ is not equal to the sum of the probability, but to the absolute value of the square of probabilities, $\frac{1}{\sqrt{2}}|c_n^1 + c_n^2|^2$. This inequality is the result of interference between two state vectors, because of the term $c_n^1 * c_n^2$ is not zero. Superposition in quantum mechanics means that the system, like electrons in atoms, can exist in many states. One could say that these are more posibilities than actualities because only when we measure the state of the system quantum possibility becomes actuality.

On a practical side, atomic ensembles prepared in a superposition of long-lived atomic levels, with a long coherence time, are very important for high precision spectroscopy, particularly for primary standards of time and frequency. Superposition among atomic levels is important for quantum information where quantum bits or qubits are simultaneously in an arbitrary

superposition of two states, and in this way memory and processing capabilities of quantum computers exponentially increase with the number of qubits. Quantum entanglement is also important for quantum computation and quantum cryptography. Such states in quantum metrology significantly improve the signal-to-noise ratio and the detection efficiency of the quantum state. It is a superposition and entanglement of particles that allow a quantum computer to do operations that a classical computer cannot.

Ramsey interferometric techniques used for measuring frequency (or energy) between two atomic levels by the control of the phase of the superposition of atomic energy levels, brought a great improvement in precision spectroscopy. Ramsey's method involves separate excitation pulses, the first pulse creates a coherent superposition of the long-lived levels which preceses in a magnetic field, and the next pulse at the same frequency as the first pulse probes the phase of the atomic coherence. In the space between two pulses, excitation signal acquires phase in respect to atomic coherence which depends on the detuning of the laser frequency from the unperturbed atomic transition. The method has revolutionized precise spectroscopic measurements, especially in the development of atomic clocks.

This lecture has three examples of superposition of atomic levels that allowed narrow atomic resonance for atomic standards in legal metrology and for the precise manipulation of atomic levels in a quantum computer. The examples show the importance of applying Ramsey's method of separated pulses, on the shape and width of the atomic resonance. First, I will show the application of two photon, microwave-optical spectroscopy of extremely accurate measurements of the splitting of hyperfine levels of $^{113}Cd^{+}$ions and characterize the atomic clock based on this hyperfine transition in Cd^{+}. The second part will show the implementation of CNOT quantum logic gate. In the last section I will describe the quantum phenomena of induced electromagnetic transparency (EIT) as a result of coherent superposition of Zeeman levels.

2. *Precise determination of the energy difference of the ground state hyperfine levels of cadmium ions,* $^{113}\mathbf{Cd}^{+}$

In this work [2] we show the precise measurements of the energy spacing of the two hyperfine states of cadmium ion $^{113}Cd^{+}$. The measuring principle is similar to the principles of an atomic clock, so this work is also towards the development of the atomic clock operating at 15.2 GHz, which is the energy splitting of two hyperfine levels. $^{113}Cd^{+}$ ions are trapped in a radio-frequency ion trap. Optical pumping and detection of atomic state was

performed by the radiation from the Cd lamps, which we develop for this purpose. The lamp is a glass cell with a several mg of cadmium (isotope 106) and about 1 Torr of argon. Radio frequency (RF) discharge in the lamp is induced by rf antenna and the radiation spectrum has atomic and ionic lines of ^{106}Cd. Scheme of the relevant energy levels for the ^{113}Cd $^{+}$and ^{106}Cd $^{+}$show which emission lines from the rf ^{106}Cd lamp are used for optical pumping of ions ^{113}Cd

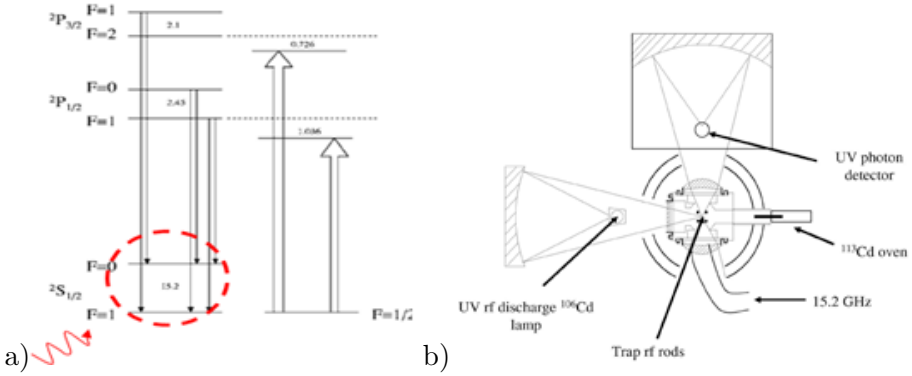

Fig. 1. a) Energy levels of the two isotopes of cadmium ions, 113 (left side) and 106 (right side). Emission from $^{106}Cd^{+}$ is used for optical pumping into the level $^{2}S_{1/2}$, F=0, $^{113}Cd^{+}$ions and detection of atomic level after the microwave interrogation. b) Schematic of the rf ion trap in the vacuum chamber with the ^{113}Cd oven and mirrors for focusing the rf lamp radiation on the cloud of ions and for the detection of scattered light by the photomultiplier

$^{113}Cd^{+}$ ions are produced in the vacuum chamber, by electron ionization of Cd atoms after vaporizing a small piece ($\sim$ 5) of ^{113}Cd, by heating the oven to about 80 ^{0}C. Ions are slowed by collisions with He atoms as a buffer gas, and trapped in the quadrupole rf ion trap with 4 rods of molybdenum, placed equidistantly along a circle with a diameter of 1 cm. Capture of ions along the radial distance from the trap axes is achieved by rf potential with the amplitude of 150 V at 1.05 MHz. Pair of electrodes opposite each other are on the same potencial, different form the potential on the other pair by the phase π. Axial capture is by dc potential at the electrodes end caps. With this rf potential and the trap geometry the secular ion oscillation frequency is about 2 π $*$ 25 kHz. Buffer gas in the vacuum chamber has a dual role in the experiment, to assist in loading the trap, and to reduce the amplitude of ion oscillations in the trap. Cloud of trapped ions has about

a million ions. Microwave radiation at about 15.2 GHz enters the vacuum chamber through a glass window and in the direction nearly perpendicular to the axis of the trap. To focus ultraviolet light from the ^{106} Cd lamp at the center of the trap and to collect the light scattered from the ions on the photomultiplier, we used a pair of large 6 inches diameter mirrors. The mirrors have a special coating to make a better use of the ^{106}Cd lamp for pumping $^{113}Cd^{+}$ and reduction background signal that comes from the radiation of a neutral atom ^{113}Cd

Two-photon resonance obtained by successive excitation by two photons, by a UV photon for optical pumping of Cd ions in the F = 0 state, and by a photon in the microwave region (close to hyperfine resonance (15.2 GHz)) is shown in Figure 2. Each result on the spectra (indicated by dots) in the figure was obtained as follows: 1. lamp was turned on for pumping into the F = 0 level, 2. rf lamp is off and interrogation pulse is on for coupling the hyperfine transition F = 0 - F = 1, and 3. rf lamp is on again, and the scattered light of the ion cloud is measured. This signal is proportional to the number of ^{113}Cd ions that during the microwave pulse are transferred from F = 0 to F = 1 hyperfine state. On the other hand, this number depends on the frequency of the microwave radiation. In Figure 2, a) the resonance was obtained by a single Raby pulse, when a single microwave pulse is applied for the ion interrogation and for flopping it from one hyperfine level to another.

Resonances for the transition between hyperfine levels F=0, m_f=0 – F=1, m_f=0 in Fig. 2, were obtained by the π polarized component of the microwave radiation, which couples magnetic sublevels with $\Delta m_f = 0$. This, so called clock transition, is not sensitive (to a first order) to external magnetic field. Width of the Rabi resonance depends on intensity and stability of microwave radiation, and on the duration of the Rabi pulse. For the pulse of 5 s, resonance width is 0.17 s, which is close to the theoretical limit given by the relation $\triangle f = 0.8/T_M$ where T_M is length of the microwave pulse. In Figs 2 b) and c) resonances are obtained after application of Ramsey resonance technique of separated excitation fields. The difference in the width of the resonances in two figures is due to the different length of time between the two pulses. For Fig. 2 b) that time is 3 s, and for data in Fig. 2 c) it is 6 s. Width of Ramey fringes in Fig. 2 c) is 0.08 s, which is consistent with the relation valid for the Ramsey method, $\Delta f = 1/2T_l$, where T_l is the interval between two microwave pulses.

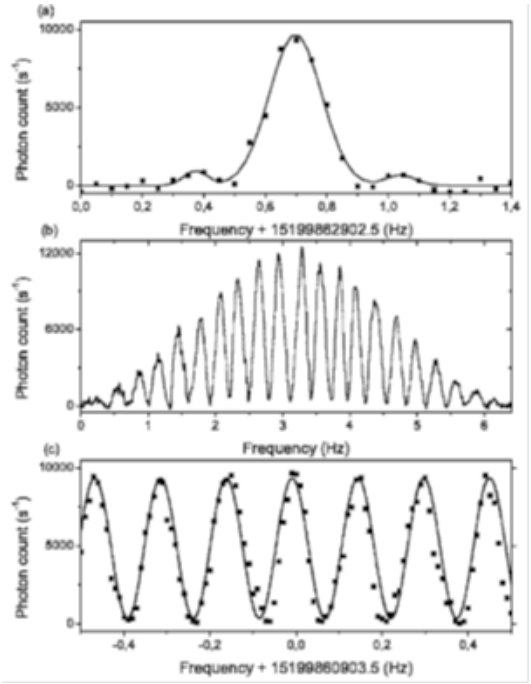

Fig. 2. The two photon F=0, m_f=0 – F=1, m_f=0 resonance, obtained using an optical photon for pumping into F=0 hyperfine level, and by scanning the frequency of microwave photon. a) Rabi resonance when the single interrogation pulse of 5 s is applyed; b) and c) Ramsey fringes obtained by the successive application of two microwave excitation pulse 0.3 s long, and separated by the pulse off time, 3 s and 6 s long, respectively

From narrow Ramsey resonances presented in Fig. 2 c), the hyperfine splitting of energy levels can be accurately measured. Our result for the difference between two hyperfine energy levels of $^{113}Cd^+$ ion, F=1 and F=0, is ν_0=15 199 862 855 (0.2). This was, at the time of the measurements, the most accurate measurements of the hyperfine splitting of ^{113}Cd+ ion. When this result is compared with other results [3] the difference is about 3 Hz, but the error of our measurements is an order of magnitude smaller. The main source of error in this measuremnts is the accuracy with which we determined the external magnetic field.

Atomic clock based on narrow Ramsey central fringe, obtained with the 6 s interval between two interrogation pulses which are 0.5 s long, would have short term stability of the order of $\sim 2 \times 10^{-13}\tau^{-1/2}$ Some features of

^{113}Cd ions trapped in the rf ion trap makes this system very attractive as a new microwave frequency standard.

3. *Experimental realization of quantum logic circuits NE*

In the work [4] we have demonstrated a quantum logic CNOT gate using quantum bits, or qubits. The quantum logic is demonstrated on the single ion $^{9}Be^{+}$, trapped in the rf Poul trap. This CNOT gate is a paradigm of quantum computing because sufficient for universal quantum computation is CNOT operation plus a simple qubit rotation. In CNOT gate on a single ion, quantum entanglement between internal atomic state and motional state are crucial for the gate operation. In the logic of this gate, the results of the gate operation on a target qubit (remains in the same state or is flipped in second state) depends on the state of the control qubit.

Trapped ions are spatially arranged in an ion trap by simultaneous actions of electrical forces and mutually repulsive Coulomb forces. If ions are laser cooled, and if the radial modes are at higher frequencies than axial modes, then ions form a crystalline array in which the oscillation of the ions is described by the normal modes of the harmonic oscillator. Number of oscillating modes is proportional to the number of ions in the trap. Construction of the ion trap allows multiple laser beams to interact with the trapped ions. The use of tightly focused laser beams allows us to address and manipulate individual ions. Lasers are used to cool ions, to optically pump ions in specific initial state, and to perform number of laser interactions to generate a superposition and entanglement for quantum logic gate.

Qubits in this experiment are internal states of ion and ion state of motion. The internal state are the two hyperfine states of the ground state $^{9}Be^{+}$. These hyperfine states are suitable as qubits for quantum operations because they are long-lived and are relatively immune to external perturbations.

The internal state of ions in the harmonic rf trap are "dressed" by quantized state of motion $|n\rangle$ of the harmonic oscillations along the axis of the ion trap. Two state of motions are two control qubits in the CNOT quantum logic gate.

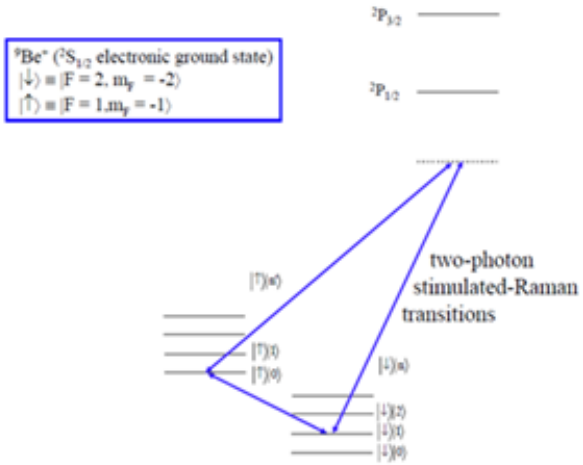

Fig. 3. Schematic of atomic energy levels of $^9B^+$ ions in the rf trap. The internal states of the ions are $|\downarrow\rangle \rightarrow |F=1,m_f=1\rangle$ and $|\uparrow\rangle = |F=2, m_f =2\rangle$ where F is one of the two hyperfine levels of the ground state $^2S_{1/2}$, and m_f is magnetic sublevel. Hyperfine states are separated by $\omega_0 = 2\pi \times 1.25$ GHz. Internal states (hyperfine states) of ions are split to motional states, separated by ω_m where m is the particular motional mode of the ion in the the harmonic rf trap

Figure 3 shows the energy diagram of electronic states, hyperfine levels and Zeeman sublevels of $^9Be^+$ ions, that are important for the CNOT quantum gate. Hyperfine states F=1 and F=2 are coupled using two lasers in Raman resonance with these atomic levels. Frequencies of Raman lasers are either tuned to the transition $^2S-^2P_{3/2}$(carrier), or detuned by one motional quanta below (red detuning) or above resonance (blue detuning). Levels coupled by Raman lasers, labeled with $|\downarrow\rangle$ $|\uparrow\rangle$ are the sublevels of the two hyper-fine levels of the ground state Be^+: $|\downarrow\rangle \rightarrow |F=1, m_f =1\rangle$,$|\uparrow\rangle = |F=2, m_f =2\rangle$. In the CNOT gate the control qubit $|n\rangle$ is a quantum state of the axial modes of the harmonic oscillator. The frequency of oscillation of the ions in this mode is ω_z. Thus, when the difference of the Raman lasers is $\omega \pm \Delta n\, \omega_z$, ion changes both the internal state (spin) and the state of motion, $|\downarrow> |n> \leftrightarrow |\uparrow> |n\, \Delta n>$.

This CNOT quantum gate is based on varying degrees of overlap of wave packets of atoms, in different states of motion, and the laser field. This is illustrated in Figure 4 when the motional states are n=0 and n=10. This means that the Rabi frequency and speed with which laser field flips the

hyperfine level depends on motional state and is larger if an ion is in n=0. For the realization of CNOT logic gate two such states of motion are | n = 0> and | n = 2>, or Δn = 2. Rabi frequency for n = 2 vibrational state of motion is lower than for n = 0 because as spatially larger its overlapping with the electric field of the laser is smaller. The realization of this quantum logic gate by using the effective difference in the size of two quantum states is also a manifestation that an ion in the trap can be represented as a wave packets of a different size.

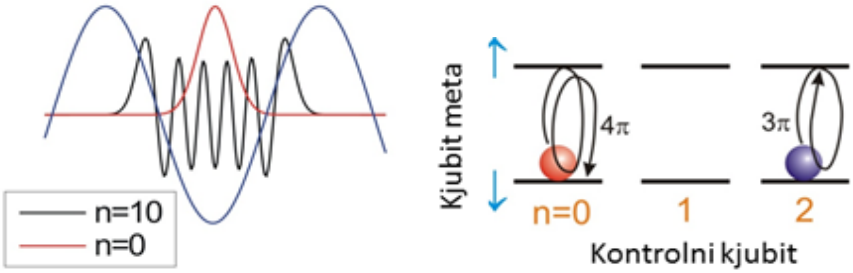

Fig. 4. Left: Illustration of different degrees of overlap of wave packets of two modes of motian, $|n = 0\rangle$ (Red line) and $|n = 10\rangle$ (Black line) and the laser electric field (blue line). Right: Schematic operation of CNOT logic gate with two qubits, one qubit is the internal state and the second qubit is the motional state. With n we marked vibrational levels due to the motion in the trap. Up / down arrows are symbolic representation for internal states of ions, as defined in the text.

Strength of the ion trap, that is the frequency of axial mode ω_z, can be adjusted by the amplitude of the rf potential applied to the trap rf electrodes. By changing the trap frequency we also change the value of the Lamb-Dike parameter $\eta = \Delta k_Z \sqrt{\frac{\hbar}{2m\omega_Z}}$. Here is Δk$_z$ is the difference of wave vectors of two Raman lasers. For the CNOT gate, the ratio of Rubi frequencies for transitions $|\downarrow\rangle|n = 0\rangle \leftrightarrow |\uparrow\rangle|n = 0\rangle$ and $|\downarrow\rangle|n = 2\rangle \leftrightarrow |\uparrow\rangle|n = 2\rangle$ is given by $\frac{\Omega_{0,0}}{\Omega_{2,2}} = 2/(2-4\eta^2+\eta^4)$. By adjusting the parameters of the ion trap, η can have a value η=0.359, for which we have $\Omega_{00}/\Omega_{22} = 4/3$. Raman lasers operating on both transitions during the gate time t_{lk} are able to make two full Rubi flopping if initial state of ion is in $|n = 0\rangle$ (so called 4 π pulse), and only 1.5 Rubi cycles if ion initially is in $|n = 2\rangle$ (or 3 π pulse). This is schematically illustrated in the right part of the Figure 4. The target qubit (internal state or spin) will change only if the control qubit (state of motion)

is in $|n = 2\rangle$, while it remains unchanged if the motional state before the gate operation is $|n = 0\rangle$.

The initial state for all CNOT gate operations is $|\downarrow\rangle|0\rangle$. In order to move the ion to that state it is necessary to perform Doppler laser cooling followed by the side-band laser cooling, i.e. to cool ion into the ground motional state, n=0. The input state of the logic gate is set by series of Raman laser pulses that are in resonance with atomic or with atomic and different motional state, i.e., they are tuned to atomic resonance, Δn = 0 (state of motion does not change) or are detuned from the atomic resonance by the motional quant Δn = $\pm$ 1. From the $|\downarrow\rangle|0\rangle$ state we come to different input states to the CNOT gate by performing series of laser operations on $|\downarrow\rangle|0\rangle$: $|\uparrow\rangle|0\rangle$ is generated by applying carrier pulses of Raman lasers, $|\downarrow\rangle|2\rangle$ is generated by the π pulse on the blue sideband ($\Delta n = +1$) followed by the π pulse on the red sideband (Δn = -1), and the state $|n = 0\rangle$ is realized by the pulse tuned to the second blue sideband resonance ($\Delta n = +2$).

After the logic gate operation during t_{lk}, state detection and determination of targets qubits follows. For detection of the ion internal state we use detection laser, that is the laser tuned to the cyclic transition $|\downarrow\rangle \rightarrow^2 P_{3/2}(F = 3, m_F = 3)$. If the ion is in the state $|\downarrow\rangle$ it scatters a large number of photons from the detection laser light. Conversely, if after the logic gate operation the ion is in state | ↑> state, virtually no photons are scattered and the detector signal is reduced to its noise level. This is a unique kind of state detection of ions, with nearly 100% efficiency

The efficiency of generating CNOT gate was $\geq$ 95% for any input state of qubits. The result of these measurements is the CNOT logic gate truth table (Figure 7) where the data are measured probabilities that after the gate operation the ion in the state —↓¿, for different gate inputs. The table shows that the initial state | ↓> | 0> remains unchanged, with probability 99/%, when the initial state is | ↓> | 0>, but is flipped by a high probability if the initial state is | ↓> | 2>. Lower row of the truth table, related to the initial state being the spin | ↓> state shows that ion remains in that state only for the input state | ↑> | 2>. Errors in generating truth table of the order of $\pm$ 0.968 are mainly due to uncertainties in preparation of the input state. Each result is the mean value of 200 individual measurements with the same input state in the gate operations.

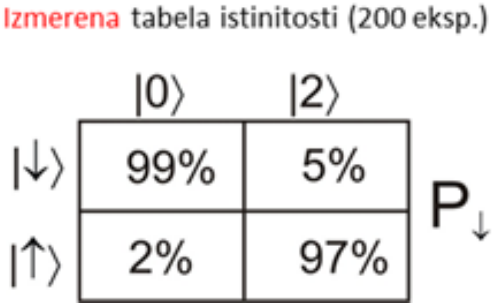

Fig. 5. Truth table for the quantum logic CNOT gate prepared by the two qubits represented by the internal state of ions (target qubit), and by two motional states (control qubit) of the same Be^+ ion.

4. *Electromagnetic induced transparency in Rb atomic vapor*

Electromagnetic induced transparency (EIT) is a coherent phenomenon that occurs when a laser(s) pump atoms in a dark state, a coherent superposition of atomic levels of which at least one is not interacting with the same laser(s). Atomic scheme necessary to induce EIT is a Λ scheme in which lasers coupled two long-lived excited levels to common excited level. Two lower levels are either two hyperfine levels of alkali atoms in the ground state, or two magnetic sublevels of the same ground state hyperfine level. EIT is manifested as a narrow resonance in the transmission of a resonant laser tuned to one of the legs of the Λ scheme. Basically, this phenomena will make medium that is opaque for a resonant laser light transparent within the narrow spectral range of Raman resonance.

Narrow EIT resonances obtained in relatively simple atomic systems like a small vapor cell, are used in a highly sensitive atomic magnetometers and atomic frequency standards and atomic clocks, in quantum information science. High dispersion within the spectral band of EIT resonance makes the medium with induced EIT suitable for studding slow light and storage of light phenomena.

In several papers [5] we investigated the behavior of EIT in Rb cell after applying Ramsey method of separated excitation regions, i.e., instead of a single Rubi pulse for atomic excitation we allow atom to experience two excitation pulses, separated by the dark period of no laser light. Influence of Ramsey effect on narrowing the EIT resonances in alkali atoms has been investigated recently, both by spatially and in time separated excitation pulses [6]. Significant effect on EIT linewidths was demonstrated

with separate excitation by the pump and probe pulse when alkali atoms are in the cell with buffer gas, usually with Ne or Ar at a pressure of several Torr. Buffer gas cells with alkaline atoms allow considerably narrower EIT resonance because the time that the atom spends in the laser beam is by an order of magnitude longer then in a vacuum gas cell. As the main factor for the decoherence of the dark quantum state is the time that atoms spend in the laser beam, EIT resonances in a buffer gas cells can be as narrow as tens of Hz. There have been attempts [6] to demonstrate Ramsey method in vacuum Rb cells (no buffer gas) by spatially separating pump laser that generates a dark superposition state, and probe laser, by a few mm. In this method probe is scattered on the atomic coherence generated in the remote pump and the whole effect depends on the amount of flux of atomic coherence that is reaching the probe. When the tow parallel lasers separated by a few mm were used like in [6], the effect was very small.

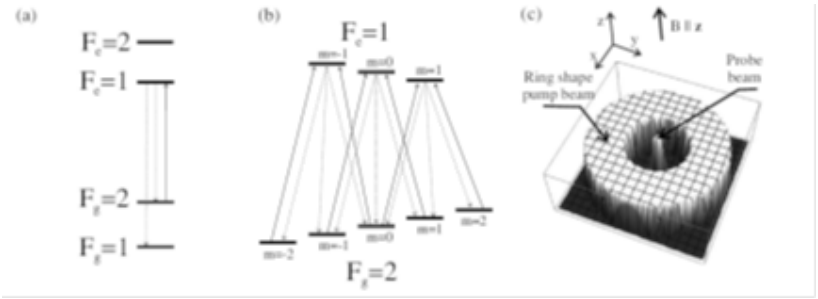

Fig 6. a) The scheme of atomic levels of ^{87}Rb D1 lines, b) energy level diagram of magnetic sublevels of hyperfine levels Fg=2 → Fe=1, c) radial distribution of the intensity of the pump (in the form of the hollow cylinder) and the probe (Gaussian intensity profile)

In [5] we use the special geometry for the pump and the probe laser to increase the influence of Ramsey methods on the width of the EIT resonance. The pump and the probe are obtained from the same laser beam (extended cavity diode laser) which is linearly polarized and tuned to the transition $F_g = 2 - F_e = 1$ where $F_{g,e}$are hyperfine levels of the ground ^{2}S and the excited $^2P_{1/2}$state as shown in Figures 6 a) and b). Figure 6 c) shows the geometry of both beams, the pump is in the form of hollow cylinder while the probe is Gaussian beam that propagates through the pump center. Such beam geometry is achieved by 90^0 reflection of the expended pump beam on

the mirror with a hole in the middle. The probe laser beam passes through the center of the ring.

In addition to the experiment we made theoretical model to calculate Zeeman and optical coherences in the ground and the excited state, and the population of levels. Density matrix formalism of optical Bloch equation is used to obtain these parameters. The total population of the Zeeman sublevels of the excited hyperfine levels, averaged over the directions of atom motion and velocity, is compared with the measured transmission of the probe laser.

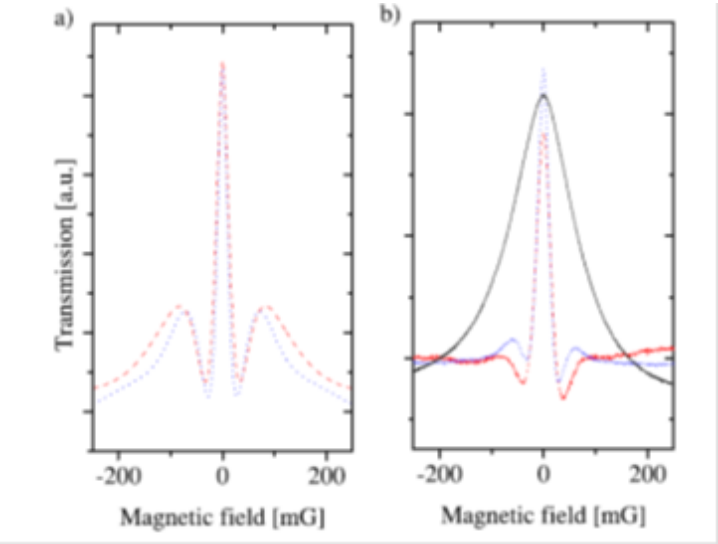

Fig. 7. Calculated a) and measured b) transmission of the probe laser when both probe and the pump laser are locked to the transition F = 2 – F = 1 in Rb atom, as a function of the external magnetic field. The dashed and dotted curves are for two lengths of the dark space, i.e., the distance between the pump and the probe, 1.7 and 2.7 mm, respectively. The broader resonance, shown by a solid line was obtained when the pump is turned off, for the same probe intensity of 10 μW. The intensity of the pump is 0:55 mW.

In Figure 7, we give comparison between theoretical (a) and experimental (b) results for the transmission of the probe that passes through the center of the hollow pump. The intensity of the probe is weak so that the perturbation of atomic coherence due to the probe is negligible. Solid line in Figure 7 b)

shows probe EIT when the pump is turned off. Ramsey effect is manifested by considerable narrowing of the EIT and Ramsey like fringes on the EIT waveforms, The central fringe (B=0) is by far the most pronounced, the others are much weaker due to wide velocity distribution of atoms. The good agreement between theory and experiment are evident.

REFERENCES

[1] N. Ramsey, *Molecular beams (Oxford University Press,* London, 1956)

[2] B. M. Jelenkovi et al., Phzs. Rev. A 74, 022505 (2006).

[3] U. Tanaka, H. Imajo, K. Hayasaka, R. Ohmukai, M. Watanabe, and S. Urabe, Phys. Rev. A 53, 33985 (1996).

[4] De Marco et. al. Phys. Rev. Let. 89, 267901 (2002).

[5] Z. D. Grujić et al., Phys. Rev. A 78, 063816 (2008).

[6] A. S. Zibrov and A. B. Matsko, Phys. Rev. A 65, 013814 (2001).

Institute of Physics
Pregrevica 119
11080 Zemun – Beograd
Serbia